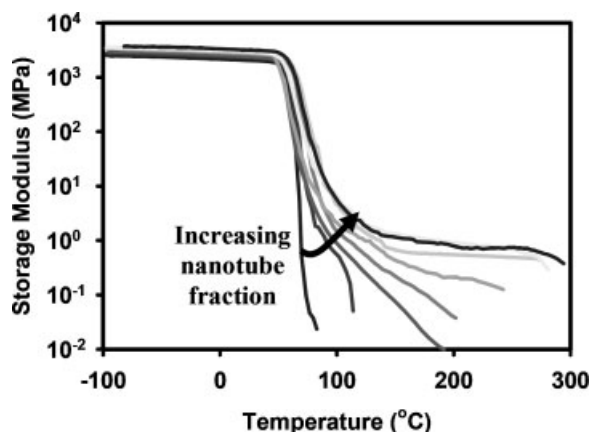


Composites of Single-Walled Carbon Nanotubes and Styrene-Isoprene Copolymer Latices

Mai L. P. Ha, Brian P. Grady,* Giulio Lolli, Daniel E. Resasco, Warren T. Ford

Composites of a styrene-isoprene copolymer and SWNTs were prepared by emulsion and miniemulsion polymerization in the presence of SWNTs, as well as by mixing dispersed SWNTs with a styrene-isoprene copolymer latex after polymerization. For the former, the surfactant was displaced from SWNTs to monomer droplets leading to SWNT aggregation. Mixing dispersed SWNTs with latex after reaction was able to preserve SWNT dispersion and gave a polymer composite with an electrical percolation threshold of 0.2%. Dynamic mechanical measurements of film samples in tension showed that the composites had a measurable modulus above T_g , indicating entanglement formation. The modulus above T_g was strongly temperature dependent, confirming shear measurements that have shown entanglements in SWNT/polymer composites involve both polymer and nanotubes.



Introduction

Fifteen years from the date Iijima reported about the existence of carbon nanotubes^[1] (CNTs), enormous progress has been made in their understanding, production, and application. There are two main types of CNTs: multi-walled nanotubes (MWNTs), which are composed of many different radii concentric tubes, and single-walled

nanotubes (SWNTs). Diameter of CNTs varies over 1.4–100 nm for MWNTs and 0.4–3 nm for SWNTs. Their aspect ratio can be 1 000 or more. Reported tensile strength and modulus range over 11–150 and 270–1 470 GPa, respectively.^[2–4] The fact that electrical properties of SWNTs are much better than MWNTs and the fact that inner tubes of MWNTs do not contribute significantly to some mechanical properties make SWNTs more attractive for certain applications.

CNTs, besides their superb mechanical properties, also have excellent electrical properties: the conductivity can be five times that of copper; and theoretically, metallic nanotubes can withstand a current 1 000 times higher than copper or silver. The thermal conductivity of SWNTs is also extremely high; higher than diamond or copper. Such properties suggest that nanotubes are an excellent material to incorporate with polymers. There have been an

M. L. P. Ha, B. P. Grady, G. Lolli, D. E. Resasco
School of Chemical, Biological and Materials Engineering, and
Carbon Nanotube Technology Center (CANTEC), University of
Oklahoma, Norman, OK 73019, USA

E-mail: bgrady@ou.edu

W. T. Ford

Department of Chemistry, Oklahoma State University, Stillwater,
OK, USA

extremely large number of papers involving CNTs mixed with polymers; for example, a key word search on “carbon nanotube and polymer” in Web of Science[®] yielded more than 2 500 hits for the period 2000–2005.

However, the promising characteristics of CNTs have not easily found their way into applications, partly because of the difficulty in dispersing tubes into individual units. Single-walled CNTs are especially difficult to disperse; they tend to be synthesized in the form of bundles that are difficult to separate into individual tubes due to high van der Waals interactions. Many efforts have been made to separate the tubes: (i) functionalize nanotube walls with small molecules,^[5,6] (ii) adsorb polymers^[7,8] and/or surfactants^[9,10] onto nanotubes, and (iii) disperse nanotubes in superacid^[11] or various organic solvents,^[12–14] where the attraction between solvent molecules and the tube is greater than the tube-tube interactions. These methods often yield a fraction of the individually dispersed tubes along with some fractions of bundled tubes. To further separate individual tubes, centrifugation/filtration can be used;^[15] however, a large fraction of CNTs can be wasted. Even if tubes are separated in one step of a procedure, dispersed CNTs tend to clump together if allowed to reaggregate, forming a network structure which is very difficult to disperse in any environment.

A quantitative measurement of how well nanotubes are dispersed is also an issue. The percolation threshold for electrical conductivity, which measures the concentration at which a continuous network forms, is perhaps the best measure of dispersion in polymers; the lower the percolation threshold, the better the dispersion. Mitchell et al.^[16] achieved percolation at 1 vol.-% using functionalized SWNTs in polystyrene. Another group,^[17] using melt processing, achieved SWNT alignment in polyimide fibers, resulting in significantly higher tensile moduli and yield stress compared to unoriented nanocomposite film at the same SWNT content. Pöstchke,^[18] using a melt-mixing method, found percolations between 0.25 and 0.5 wt.-% SWNTs. In a SWNT-epoxy system, Barrau^[19] achieved electrical percolation of 0.08 wt.-% SWNTs. Kim et al.,^[20] using functionalized MWNTs and epoxy resin, achieved an electrical percolation threshold of 0.017–0.077 vol.-%; to the best of our knowledge the former is the lowest number reported in literature.

In general, the lower the percolation threshold, the better is the mechanical reinforcement by nanotubes. The reinforcement mechanism in the composite is based on stress transfer from polymer to nanotubes. Lower percolation thresholds mean that nanotubes are found with less aggregation. Apparently, the best stress transfer from polymer to nanotubes occurs with lower tube aggregations. Poor dispersion is most likely the explanation for many reports that do not show any significant improve-

ment in mechanical properties, some even show lower results than the pure polymers.^[21,22]

Methods that produce the lowest percolation threshold materials for SWNTs in already-formed polymers involve the use of an organic solvent that disperses the nanotubes and dissolves the polymer.^[16,23] Alternatively, a water-soluble polymer is used along with tubes that have been dispersed in water.^[24] Neither approach is very practical: the former because organic solvents are expensive and typically environmentally hazardous; the latter because a water-soluble polymer is not conducive to almost all the envisioned applications.

On the other hand, dispersing inorganic particles in a stable emulsion has been studied by many investigators because of its commercial importance, i.e., pigments in latex paints or reinforcing filler particles in polymer. An encapsulation approach can be used to produce a particle with an inorganic core and a polymer shell. The general approach is to disperse the inorganic solid, and then polymerize around the solid. The most common method, emulsion polymerization, has been used to encapsulate inorganic particles such as titanium dioxide,^[25–27] calcium carbonate,^[28] silica,^[27] aluminum,^[29] aluminum oxide,^[27] or pigments such as phthalocyanine blue pigments,^[30] and aluminum pigments.^[31] One group^[32,33] encapsulated MWNTs with butyl acrylate and methyl methacrylate (MMA), and another group^[34] has successfully dispersed carbon black by miniemulsion polymerization. Barraza et al.^[35] produced SWNT composites by miniemulsion polymerization utilizing cetyltrimethylammonium bromide (CTAB) as the surfactant, and achieved some improvement in electrical and mechanical properties. A more recent paper^[36] compared both miniemulsion and normal emulsion polymerization of polystyrene in the presence of SWNTs. The focus was on dispersability after drying of the mixture rather than the mechanical properties of the solids. Solid properties were measured on dried latex beads without surfactant extraction; the conductivities were poor while the solid properties were confounded by the use of a crosslinking agent and the fact that coagulation has a large effect on solid properties.

Another related approach is to disperse the solid in already-formed polymer latex using a simple mixing procedure.^[37] In poly(vinyl acetate) latex, Grunlan et al.^[38] reported electrical percolation at 1.6 vol.-% of carbon black; the same group reported an exceptionally low percolation threshold of 0.038 wt.-% in poly(vinyl acetate)-filled SWNT dispersed by gum arabic.^[39] Regev et al.^[40] mixed SWNTs dispersed by sodium dodecylsulfate (SDS) and gum arabic with polystyrene latex and achieved percolation at 0.28 wt.-% of SWNTs. Dufresne et al.^[41] mixed latex and MWNTs, the latter dispersed with SDS, and achieved a percolation threshold of 1.5% and saw substantial increases in Young's modulus, but the tensile strength

dropped substantially. Nevertheless, this approach could promise a flexible and environmental friendly method to produce SWNT composites.

In this paper, following the dispersion of SWNTs in SDBS as described by Matarredona et al.^[9] we employ the encapsulation method and the mixing method to produce SWNT composites. Excess surfactant was extracted and the polymer remelted to form films for characterization. Mechanical, electrical, thermal, and linear viscoelastic tests were used to characterize the films.

Experimental Part

Materials

Styrene and isoprene monomers, purchased from Sigma-Aldrich, were passed through an inhibitor removal column twice, then stored no longer than 60 d at 5 °C before use. 2,2'-Azobisisobutyronitrile (AIBN) from Sigma-Aldrich and SDBS, 95% purity, were used as received. Hexadecane, 99% purity from Alfa Aesar, was the hydrophobe in the miniemulsion experiments. SWNTs produced by the CoMoCAT[®] method,^[42] grade S-P90-02-GEL were provided by Southwest Nanotechnologies. These nanotubes having an average diameter of ≈ 0.8 nm, were pretreated in HF, filtered, and thoroughly washed in deionized water. All the solutions were prepared with deionized water.

Emulsion Polymerization in the Presence of Nanotubes

Recipes used for formulation are given in Table 1. SWNTs were dispersed by ultrasonication for 1 h following the method developed previously.^[9] AIBN was then mixed with the SWNT-surfactant solution. The monomer (and hydrophobe, in miniemulsion cases) was added and the whole mixture was stirred at room temperature for 1 h. In the case of no nanotubes, only one solution was employed and AIBN was added with the monomer. After 1 h of stirring, the flask was sonicated for 60 s and, imme-

diately after sonication, the mixed solution was stirred at 65 °C for 14 h. Water was evaporated and the remaining solid polymer was extracted with isopropyl alcohol using a Soxhlet apparatus to remove the hexadecane and the surfactant. The resulting product was then dried to remove the isopropyl alcohol.

Samples A-0, A-0.5, and A-1.0 are macroemulsions with 0, 0.5, and 1.0 wt.-% SWNTs, respectively. Samples I-0, I-0.5, I-1.0, and I-2.0 are miniemulsions with 0, 0.5, 1.0, and 2.0 wt.-% SWNTs, respectively. The amount of SDBS in the emulsion polymerization without SWNTs is 6×10^{-3} M (5 cmc). In the composite samples, SDBS amount is the amount needed to adsorb on the walls of SWNTs according to the adsorption isotherm^[9] $+ 6 \times 10^{-3}$ M. As Table 1 indicates, by comparing the amount of surfactant in samples with and without nanotubes, the amount of surfactant adsorbed on nanotubes is much greater than the amount of surfactant in solution or part of micelles due to the large surface area of the nanotubes. The oil/water phase mass ratio is 10:90 in both types of reactions. In miniemulsion cases, the hydrophobe is 5 vol.-% of the monomer.

Mixing Latex and Nanotubes

The starting surfactant solution concentration was 8.4×10^{-3} M while the concentration of SWNTs was $0.1 \text{ mg} \cdot \text{mL}^{-1}$ yielding a surfactant concentration after adsorption according to the adsorption isotherm^[9] of about 0.9×10^{-3} M (0.75 cmc). Vials containing 25 mL of the mixture were sonicated for 1 h. The latex was produced by macro- and miniemulsion polymerization processes without SWNTs (A-0 and I-0). The unprocessed product was used, i.e., no drying. The SWNT dispersion was then mixed with latex in a beaker by stirring at room temperature for 20 min; no vigorous means of homogenization such as ultrasonication was used during mixing. The same batches of latex from macro- and miniemulsion polymerization were used throughout this experiment to eliminate batch-to-batch error. The volume ratios of the SWNT solution and the latex were varied to control the SWNT content of the final product. After drying, the solid sample was extracted using a Soxhlet apparatus and dried as described previously. Table 2 shows the substantial drop in surfactant

Table 1. Emulsion polymerization recipe.

	Water	SDBS	SWNT	Styrene	Isoprene	AIBN	Hexadecane
	mL	g	g	g	g	g	mL
A-0	180	0.376	0	16.45	3.6	0.25	0
A-0.5	180	2.725	0.1	16.45	3.6	0.25	0
A-1.0	180	5.074	0.2	16.45	3.6	0.25	0
I-0	180	0.376	0	16.45	3.6	0.25	1.2
I-0.5	180	2.725	0.1	16.45	3.6	0.25	1.2
I-1.0	180	5.074	0.2	16.45	3.6	0.25	1.2
I-2.0	180	9.771	0.4	16.45	3.6	0.25	1.2

Table 2. SDBS content in composites before and after extraction.

SWNT content	SDBS content before extraction	SDBS content after extraction
%	%	%
0	4.49	0.57
1	27.98	3.7
2	50.6	5

concentration in the polymer after extraction and emphasizes the importance of the extraction step.

Analytical Methods

Molecular weights were measured with a Water 490 Gel Permeation Chromatograph with tetrahydrofuran (THF) solvent, using polystyrene calibration standards. Latex sphere sizes were observed from scanning electron microscope (SEM) Joel 880 and transmission electron microscope (TEM) Zeiss 10 images. The dispersion of SWNTs was evaluated by IR absorption with a Bruker Equinox 55. Samples for mechanical test were prepared by hot pressing and cut by the desired mold. Tensile tests were performed by United STM-2K tensile tester at the rate of $0.25 \text{ cm} \cdot \text{min}^{-1}$. Dynamic mechanical analysis (DMA) measurements made on a Rheometric Scientific (now part of TA Instruments) RSA II were used to determine storage and loss moduli of samples at 1 Hz. 3°C temperature steps were used with static force tracking dynamic force. Selected samples were also run in a three-point bend geometry. Glass transition temperatures (T_g s) were measured by a DSC. Electrical conductivities were tested by a two-point probe method with a specially constructed resistivity chamber, calibrated by a Keithley 610C Electrometer. The lower limit of conductivities that could be measured with this equipment was approximately $10^{-14} \text{ S} \cdot \text{cm}^{-1}$. Elemental analysis of sulfur was performed by Galbraith Laboratories to determine the amount of surfactant in the material.

Results and Discussion

Encapsulation via Emulsion Polymerization

SWNTs, in their individual (fully dispersed) state, possess well-defined optical absorption peaks due to their sharp electron energy levels. When bonded or bundled together, the graphite crystal structures are affected, resulting in broadening of the energy levels and widening of the optical absorption peaks. Hence, if the distribution of nanotube types in a sample is relatively narrow, then optical absorption can be used as a semi-quantitative means of determining nanotube dispersion. Optical absorption spectra of SWNTs dispersed by SDBS in water,

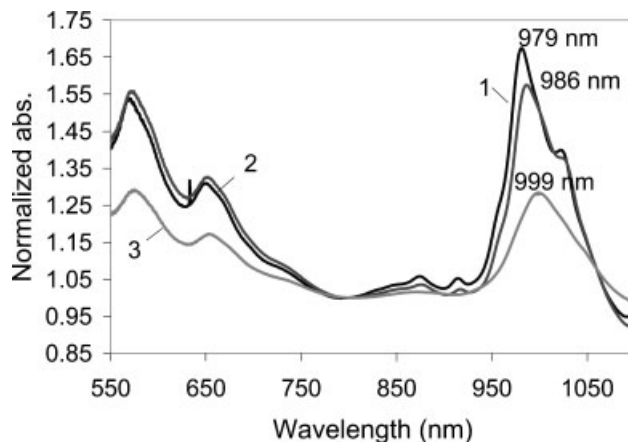
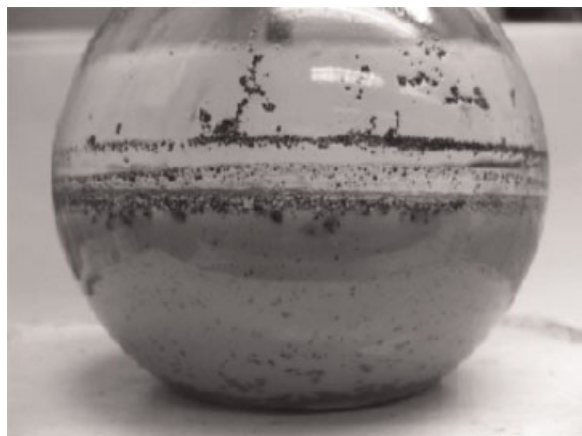


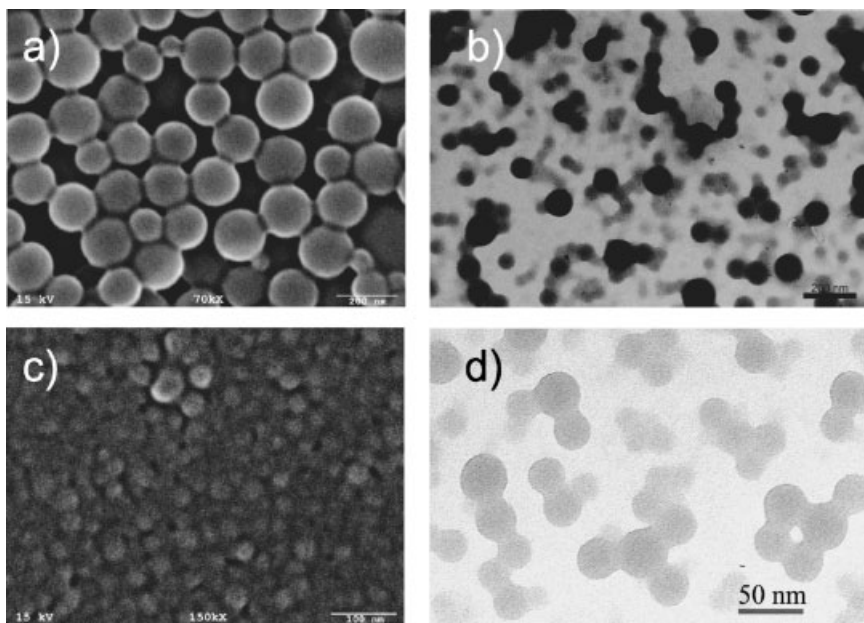
Figure 1. Optical absorption spectra after (1) SWNT dispersed by SDBS, (2) adding monomer in macroemulsion polymerization, and (3) adding monomer and hydrophobe in miniemulsion polymerization.

as shown in Figure 1, show sharp and narrow peaks at 979 and 573 nm (S11 and S22 transitions), indicating the existence of individual SWNTs, with the (6,5) type as the major component in the solution. Shoulders at 655 and 1030 nm indicate the presence of smaller amounts of (7,5) and (7,6), typically observed in CoMoCAT samples.^[43] In the composite synthesis, monomers were added to the dispersed SWNTs solution and the whole solution was stirred for 1 h (pre-emulsification step). With the normal ultrasonication step, no optical signal could be observed because of monomer droplet scattering. Without ultrasonication, the solution quickly separated into two macroscopic phases within several minutes: an oil-rich and a water-rich phase. Both were checked with optical absorption to monitor the change in the dispersion of SWNTs. In the oil-rich phase, styrene peaks dominated the signal and other absorption bands could not be discerned. In the water-rich phase, corresponding to emulsion polymerization, the SWNT peak shifted to 986 nm indicating an interaction between monomers and the nanotube. The resonance ratio, defined by the ratio of the resonant area to its nonresonant background,^[44] can be used as a semi-quantitative measure of dispersion. The resonance ratio shifted from 0.28 to 0.26 indicating perhaps that some SWNTs had reaggregated, although the drop was not large. In the water-rich phase corresponding to miniemulsion polymerization, the absorption peak was lower and broadened significantly compared to the peak in conventional emulsion polymerization; the resonance ratio dropped to 0.12 and the peak was shifted more to the right (999 nm). Peak shifting implied a stronger interaction between monomer and SWNTs, but the lower resonance ratio clearly indicated reaggregation. In other words, the more hydrophobic the oil phase, the less dispersed the SWNTs are in the water phase.



■ Figure 2. Photograph showing appearance of SWNT clusters.

As the monomer reacted to form a polymer, the “oil phase” became more hydrophobic. Consistent with the more hydrophobic oil phase, SWNT clusters gradually became visible in both macro- and mini-emulsion polymerization (Figure 2). SWNT cluster formation suggests a loss of the stabilizing surfactant. SEM and TEM pictures show a significant reduction in latex particle size, from 100 to 20–30 nm with the addition of nanotubes in emulsion polymerization (Figure 3). The reduction in particle size implies that more surfactant is stabilizing the monomer; i.e., the reduction in particle size is consistent with surfactant migration from SWNTs to latex. The monomer, instead of diffusing between the surfactant tail and SWNT



■ Figure 3. SEM pictures of macroemulsion polymerization (a) S-I copolymer latex (scale bar 200 nm) and (c) composite latex (scale bar 100 nm). TEM pictures of miniemulsion polymerization (b) S-I copolymer latex (scale bar 200 nm) and (d) composite latex (scale bar 50 nm).

■ Table 3. Molecular weights of selected polymers.

Sample	\overline{M}_w	PD
	$\text{g} \cdot \text{mol}^{-1}$	
A-0	230 000	6.41
A-0.5	120 000	4.71
I-0	225 000	3.17
I-0.5	128 000	4.78

wall and being admicelle-polymerized as expected, caused a disruption of surfactant adsorption on SWNTs. As a result, SWNTs lost their stabilizing surfactant and returned to an aggregated state. Assuming that most of the surfactant migrated from the nanotubes to monomer-micelle droplets, then the large amount of surfactant would bring the emulsion to microemulsion polymerization conditions. Particle sizes in both the miniemulsion and normal emulsion cases (20–30 nm) were well within the microemulsion range.

As a further evidence of surfactant diffusion, weight-average molecular weight (\overline{M}_w) and polydispersity index (PD) of copolymer samples displayed in Table 3 show qualitative differences with and without nanotubes. The PDs of miniemulsion and normal emulsion polymers made without nanotubes are different, representing typical differences between these two polymerization types. If the polymerization mechanisms were different for the reactions carried out in the presence of SWNTs, then the PDs of the resulting polymers should also have been different. The fact that the PDs were the same for the samples made with nanotubes supports the conclusion that the polymerization mechanisms were the same.

Perhaps, surfactant desorption from the SWNT wall was the result of the strong interaction between the π electrons in the benzene ring of styrene and those of the nanotube's wall, i.e., the surfactant was displaced by the adsorbing styrene. Hence, the procedure was repeated with MMA; a monomer that should not have a strong interaction with nanotubes. We observed a gradual appearance of SWNT clusters as before and EM images (not shown) also indicate a significant reduction in the polymer particle size. Hence, the adsorption of monomer to the nanotubes does not appear to be the most important driving force causing the partitioning of

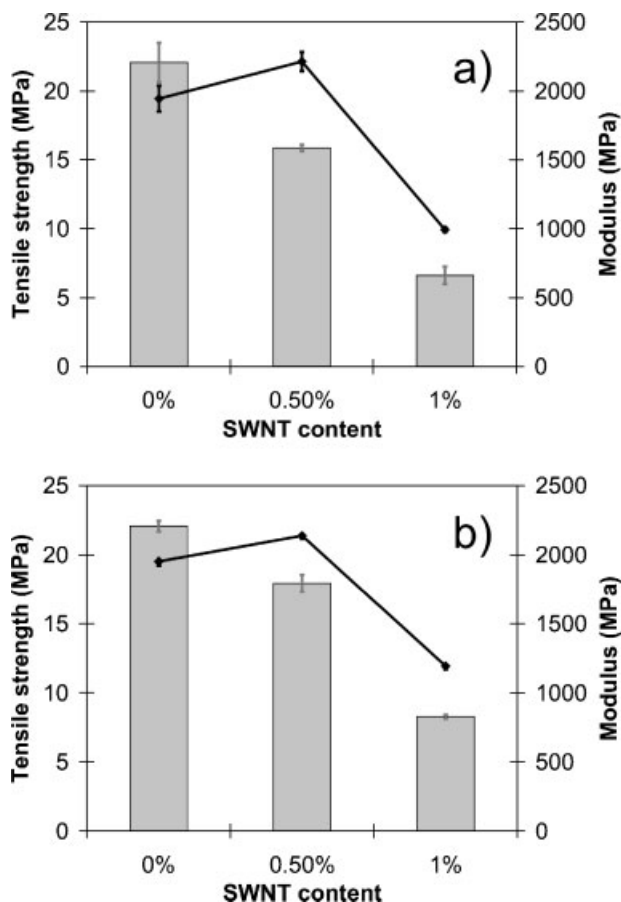


Figure 4. Mechanical properties of SWNT composite by (a) mini-emulsion polymerization (b) macroemulsion polymerization; column: tensile strength, line: modulus.

surfactant from the nanotube to the latex. Rather, small monomer drops formed during stirring have a stronger affinity for surfactant than nanotubes, and hence these otherwise unstable droplets are able to become stable via the transfer of surfactant from nanotubes to latex.

With aggregation, SWNTs are expected to play a negative role in the polymer. When encapsulated by the polymer in either of the reaction methods, SWNTs served as poor fillers in the composites, causing a significant drop in the tensile strength (Figure 4). Conductivity showed essentially no improvement in the volume fractions as high as 2%.

Mixing with Latex

During emulsion polymerization, the oil-water interfacial area is determined by the available surfactant in the solution; the results of the present study have shown that adsorbed surfactant on the surface of the nanotubes is available for the oil phase because surfactants can migrate. While in theory the same is true with the latex, the high

viscosity of the latex spheres means that breaking apart the spheres is much more difficult. Furthermore, there is very little monomer as a “mobile” component that can diffuse in between SWNT’s wall and SDBS’s tail group. Hence, simple mixing is not expected to suffer from the same surfactant mobility problems as polymerization in the presence of the tubes. We were not able to observe the optical absorption of the mixed solution due to scattering; however, we found in the optical spectrum of the solid composites that the SWNTs absorption peak had shifted to 999 nm (Figure 5) indicating an interaction between the polymer and SWNTs. The thin film was also macroscopically homogenous.

The electrical conductivity plot (Figure 6) has the expected percolation behavior and the following equation was used to fit the data:^[45]

$$\sigma \sim (m - m_{c\sigma})^{\beta\sigma} \quad (1)$$

where σ is electrical conductivity, m the SWNT mass fraction, $m_{c\sigma}$ the electrical percolation threshold, and $\beta\sigma$ the critical exponent. Mixing SWNTs dispersed in SDBS with latices produced from macroemulsion and miniemulsion polymerization gives the value of $m_{c\sigma}$ as 0.2%, while $\beta\sigma$ values are 7.55 and 7.27, respectively. The percolation threshold is close to the previous report for a SDS-PS latex system.^[40] However, in our system, salt or nondialyzed latex was not employed to reduce the repulsion between latex spheres and SWNTs. In centrifugation experiments run on the SWNT-surfactant solution immediately prior to mixing with the latices, only 65% of the SWNTs are still in solution after an hour of centrifugation at 15 000 rpm. With the almost certainly correct assumption that only suspended nanotubes contribute to continuous network formation, the actual electrical percolation threshold is

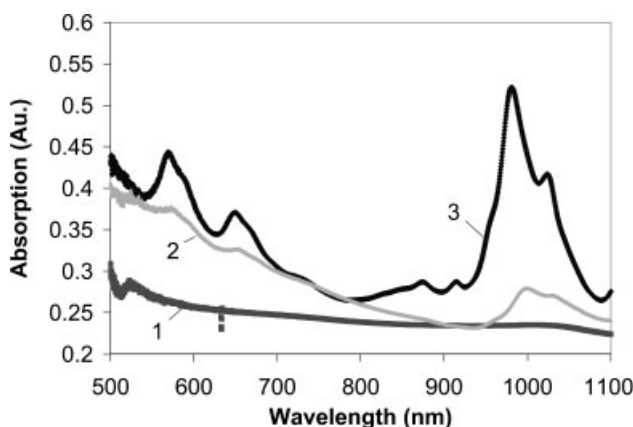


Figure 5. Optical absorption of (1) S-I copolymer thin film, (2) S-I copolymer/o.1% SWNT composite by mixing, (3) SWNT dispersed in SDBS solution.

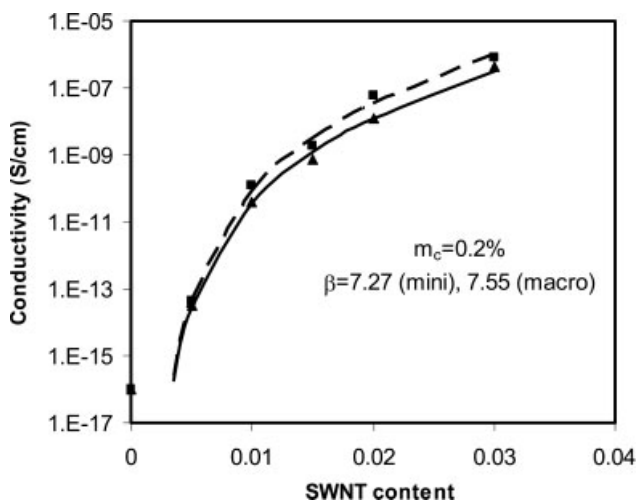


Figure 6. DC Conductivity measurement of composite film containing dispersed SWNT in S-I copolymer latex prepared from miniemulsion [■: data point, solid line: fitted curve from Equation (2)] and macroemulsion [▲: data point, dashed line: fitted curve from Equation (2)] polymerization. From 0 to 0.25 wt.-% SWNT content, conductances are out of our equipment range; hence data at 0 wt.-% are taken from the literature.^[56]

very likely near 0.13%, which is about twice the value predicted by theory^[46,47] for SWNTs with aspect ratio 2000:1 (the approximate aspect ratio of the nanotubes used in this study).

The tensile strength shows improvement at values as low as 0.1 wt.-% SWNTs. All the composite samples had an increased elongation at break compared to the pure copolymer (Figure 7). For the tensile strength and elongation at break to increase, there must be some stress transfer from polymer matrix to SWNTs. The modified mixture law of Piggott^[48] was used to model the data:

$$E = 0.2V_f E_f + V_m E_m \quad (2)$$

$$\sigma_s = 0.2V_f \sigma_{sf} + V_m \sigma_{sm} \quad (3)$$

where E is the modulus, σ_s the strength, subscript f stands for filler and m for matrix polymer. Density values of 1.3 and 1.0 g · cm⁻³, modulus values of 600 000 and 2 450 MPa, and strength values of 30 000 and 16 MPa were used for SWNTs and styrene-isoprene (S-I) copolymers respectively.

According to this model, the tensile strength and Young's modulus correspond to the theoretical value until 0.5 wt.-% of SWNTs content (Figure 8). At higher loadings, the tensile strength and elongation at break are reduced and the modulus seems essentially unaffected. Higher SWNT loadings do mean larger amounts of surfactant which could in turn negatively affect the mechanical properties; however, adding back surfactant in the pure S-I copolymer sample to levels in the higher SWNT content

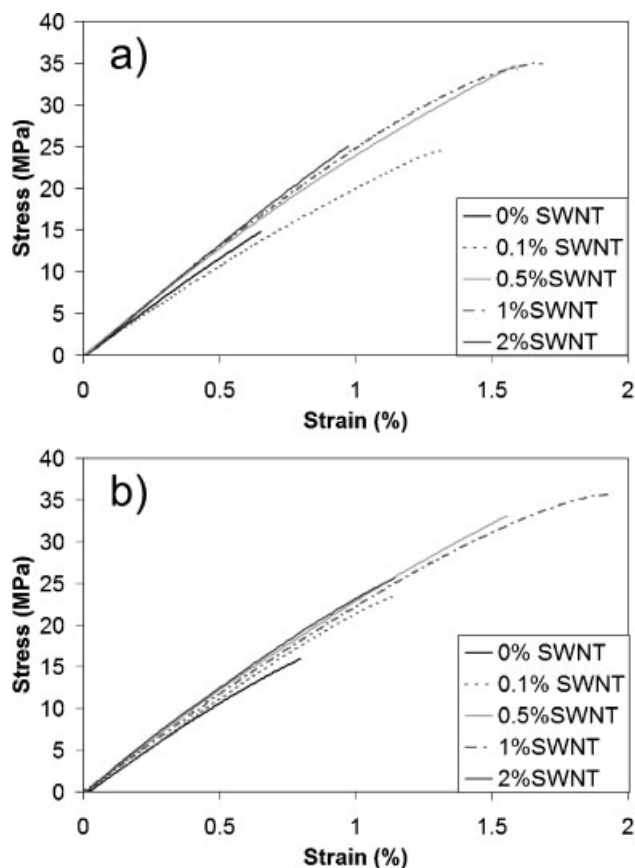


Figure 7. Typical stress-elongation curves of pure copolymer and SWNT composite (a) miniemulsion polymerization, (b) macroemulsion polymerization.

samples does not affect the mechanical properties, and hence the drop does not seem to be related to the surfactant level. Another possibility for the decreasing trend at higher SWNT content is the dispersion of SWNTs. In composite systems, even with ideal dispersion, local aggregation appears above the percolation threshold. On applying stress, these aggregates will become stress centers and initiate failures in the materials. The situation with nanotubes is expected to be worse; perhaps larger aggregates occur at higher loadings leading to reduced tensile strength and elongation at break.

Figure 9 shows DMA plots for the samples; there are a number of interesting observations about these plots. First, the storage modulus increases with the addition of nanotubes below the T_g in agreement with the Young's modulus. Secondly, at temperatures above the glass transition region, the complex modulus of composites is measurable. The only time a complex modulus is measurable in a single-phase amorphous polymer above the glass transition region in this geometry is when the material is crosslinked. In order to check whether nanotubes would be catalyzing the reaction of isoprene double

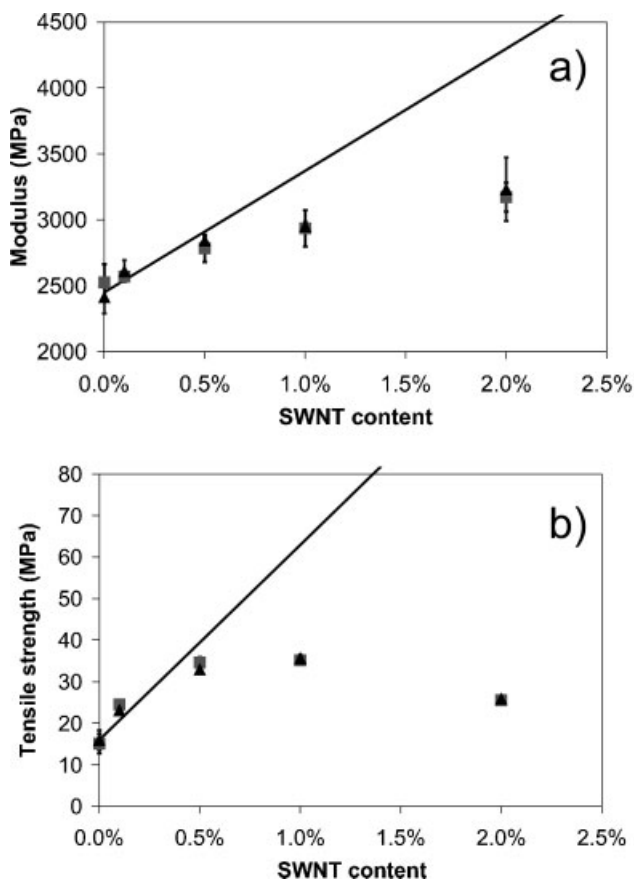


Figure 8. Theoretical prediction (line) by modified mixture law versus experimental results (■: miniemulsion, ▲: macroemulsion) of modulus (a) and tensile strength (b) measured at room temperature.

bonds leading to chemical crosslinking, polystyrene homopolymer composites were made in the same manner and the results are shown in Figure 10. Clearly, the complex modulus is measurable above the glass transition region, so the result is definitely a reinforcing effect due to the presence of the nanotubes and is not due to a chemical reaction.

The fact that the modulus is measurable in terms of tension is a consequence of geometry; in fact, a three-point bend geometry yields an immeasurable modulus above the glass transition (plot not shown). In a three-point bend, the material will be sagging due to a combination of its weight and the necessary force required for performing DMA measurements, causing an immeasurable modulus. Of course, it might be possible to choose a small enough force to prevent this sagging from happening; but the force of the last measurable data point was approximately 7×10^{-4} g, which represents the error limit of the machine.

The formation of a continuous network involving CNTs was recognized by Pötschke et al.^[49] using linear viscoelastic measurements made in shear, and has been

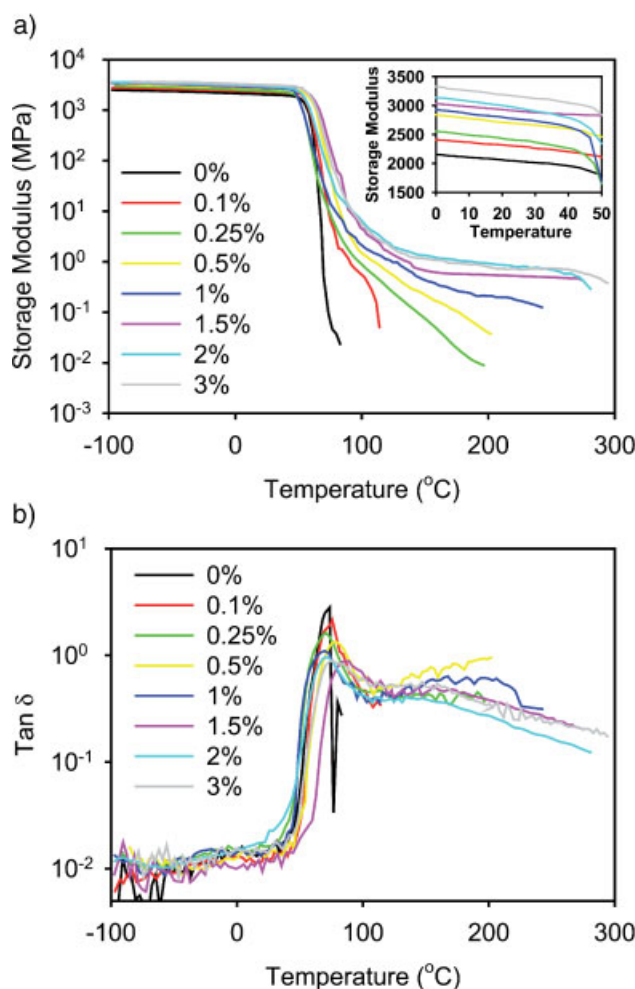


Figure 9. Storage modulus versus temperature and tan δ peak height versus temperature at different SWNT contents of SWNT/S-I copolymer composites (styrene/isoprene 75/25) measured in tension.

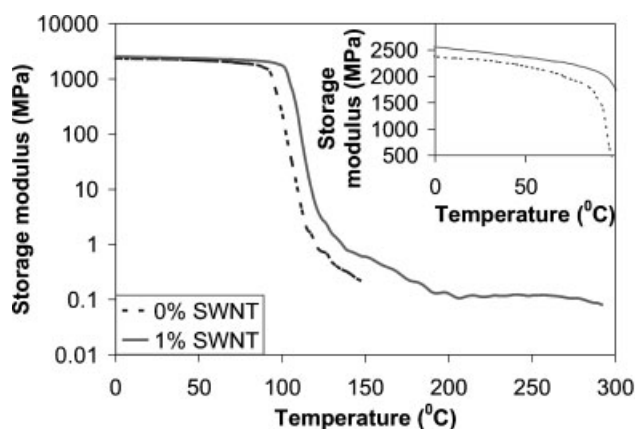


Figure 10. Storage modulus versus temperature of SWNT/polystyrene composites measured in tension.

explored by this author^[50–52] and others.^[16,24,45,53,54] The phenomenon observed here is exactly the same as that observed in shear; i.e., the measurable tensile complex modulus is an evidence of the formation of a continuous network involving CNTs. One advantage of measuring a film in tension versus a melt in shear is that the former easily enables the measurement of the directionality of network formation. These particular films have no particular orientation in the plane of the film because of the way in which they were made; however, future work in our laboratory will concentrate on how the mechanical network formation correlates to electrical network formation.

The other obvious advantage of measuring films in tension is that the temperature dependence of the continuous network is clearly highlighted; although the rheological percolation threshold was first identified in 2002,^[16,49] it was not until 2004 that the temperature dependence of the network was described for the first time.^[51] As shown in Figure 9, the material was able to maintain a measurable storage modulus at higher temperatures for higher nanotube contents. As argued previously,^[51] the temperature dependence clearly indicates that network formation involves both polymer and nanotubes since if network formation only involved the latter, then the modulus would not become immeasurable in this temperature range.

A similar power law relation as in electrical percolation determination can also be used to determine the rheological percolation:^[45]

$$E' \sim (m - m_{cE'})^{\beta} \quad (4)$$

where E' is the storage modulus, the fitted curve gives $m_{cE'} = 0.033\text{--}0.14$ wt.-% and $\beta^{E'} = 0.78\text{--}1.46$ depending on the temperature as shown in Figure 11 and Table 4.

β values of rheological and electrical curves are not comparable due to the change in electrical conductivity σ

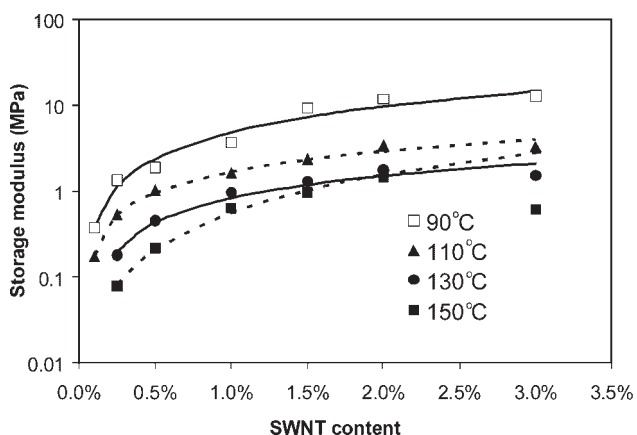


Figure 11. Storage modulus of SWNT/S-I copolymer composites at different nanotubes content measured in tension, fitted lines correspond to Equation (4).

Table 4. Rheological percolation fitting parameters at different temperatures.

Temperature °C	m_c wt.-%	β	R^2
90	0.033	0.99	0.97
110	0.08	0.78	0.99
130	0.14	0.81	0.96
150	0.055	1.46	0.92

being much larger than the change in storage modulus E' . The rheological percolation threshold at all temperatures is smaller than the conductivity percolation threshold. Rheological percolation has previously been found to be smaller than the electrical percolation as the required tube–tube distance for electrical conductivity is smaller than that for rheological percolation.^[45] The percolation threshold increases with temperature but suddenly drops at 150 °C. The fitted curve at 150 °C is unlike other fitted curves at lower temperatures, which may indicate isoprene crosslinking or degradation. Therefore, the calculated percolation value based on the fitted curve at 150 °C might not be accurate.

Glass transition temperatures measured by DSC reflect a slight drop with increasing nanotube content as shown in Figure 12. The value at 3.0 wt.-% is quite possibly an outlier, although duplicate measurements indicate that the value is reproducible. The sample-to-sample variation in the shape of the $\tan \delta$ peak (Figure 9) is quite significant, which means the variability in T_g determined from the temperature corresponding to the peak in $\tan \delta$ was ≈ 5 °C. The instrument itself is not associated with this variability; this instrument and geometry have been used to measure T_g with 1–2 °C variability. These changes are most likely associated with small changes in nanotube align-

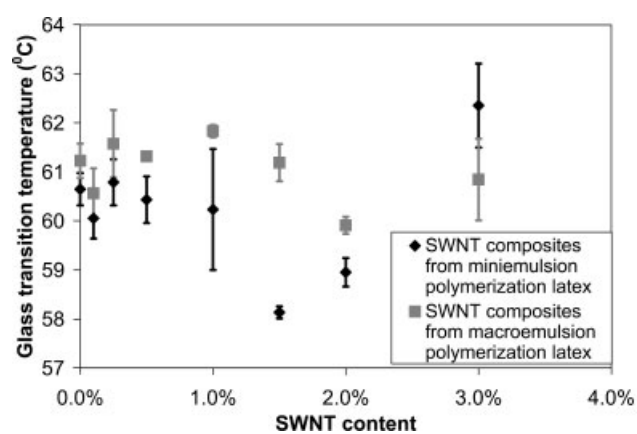


Figure 12. T_g measured by DSC versus SWNT content.

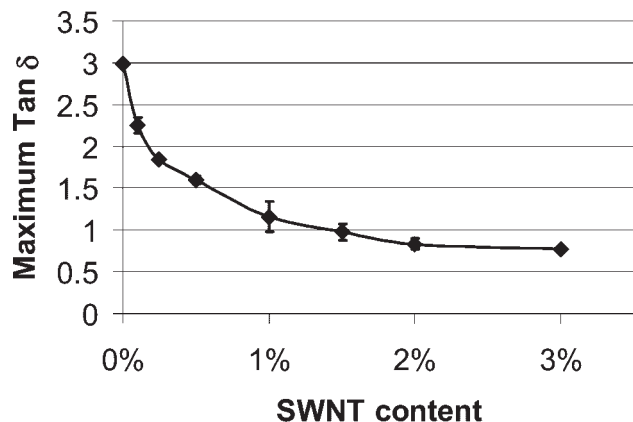


Figure 13. $\tan \delta$ at glass transition peak versus SWNT content.

ment during pressing and subsequent cooling; for example, the exact temperature and hence the viscosity at the moment pressure is applied, varies significantly. Normally, this lack of control is a minor issue; however, small changes in nanotube alignment would very likely change the temperature behavior of the polymer–nanotube network leading to the observed variation in $\tan \delta$ peak shape. This explanation is confirmed by the fact that multiple pressings of the same sample yielded different values of the temperature corresponding to the peak of $\tan \delta$.

The amount of material involved in a glass transition scales with the area under the $\tan \delta$ versus temperature curve under identical measurement conditions. As Figure 9 suggests, using the maximum $\tan \delta$ is a reasonable representation of the area, and Figure 13 shows that the height of the $\tan \delta$ peak decreases with increasing SWNTs content. The change is probably due to a reduction in the mobility of some chains to the point where they do not participate in the glass transition; these chains are likely to participate in the higher temperature transition where the complex modulus becomes immeasurable. This hypothesis is not new to polymers. Areas of restricted polymer mobility due to a localized high volume fraction of a nanoscale rigid 2nd phase, which in turn has the same effect on the $\tan \delta$ peak height and causes the existence of a second higher temperature $\tan \delta$ peak in DMA spectra, have been hypothesized to occur if the total area of restricted mobility within a given sample reaches a high enough concentration.^[55]

Conclusion

Encapsulation, i.e., polymerization in the presence of a solid filler, utilizing either miniemulsion or macroemulsion polymerization was not suitable for producing SWNT composites because of poor SWNT dispersion. Furthermore, TEM and SEM pictures indicate a significant reduc-

tion in latex particle size with the addition of nanotubes. These observations indicate that the surfactant was transferred from nanotubes to latex during the reaction; the loss of stabilizing surfactant from nanotubes led to nanotube aggregation. This result should be regarded as specific to this surfactant/nanotube combination; sufficiently strong surfactant adsorption on the nanotube surface could prevent transfer of surfactant in this manner. However, this work shows that surfactant transfer must be prevented while performing encapsulating polymerizations with CNTs in order to obtain good properties.

Mixing SWNTs dispersed in surfactant and polymer latices is simple, and applicable for many polymers. The percolation threshold is similar to what others have found for well-dispersed systems (0.2 wt.-% for electrical percolation, 0.033–0.14 wt.-% for rheological percolation). The mechanical properties improve with nanotube addition, particularly at low nanotube fractions. Above the T_g at high enough SWNT content, the composites have a measurable storage modulus in tension due to entanglements between nanotubes and polymer chains. Using DMA in tension to measure the mechanical properties of a nanotube composite film, it is possible to determine the rheological percolation threshold, its temperature dependence, and how these characteristics depend on orientation.

Acknowledgements: This research was supported by a grant from the Oklahoma State Regents for Higher Education and the Department of Energy (DoE-BES) grant no. DE-FG02-06ER64239. We are grateful to Leandro Balzano of SouthWest Nanotechnologies, Inc., for providing purified SWNTs.

Received: October 17, 2006; Revised: December 22, 2006; Accepted: January 5, 2007; DOI: 10.1002/macp.200600521

Keywords: carbon nanotubes; dispersions; latices; nanocomposites; rheology

- [1] S. Iijima, *Nature* **1991**, 354, 56.
- [2] J. P. Lu, *J. Phys. Chem. Solids* **1997**, 58, 1649.
- [3] F. Li, B. F. Cheng, G. Su, M. S. Dresselhaus, *Appl. Phys. Lett.* **2000**, 77, 3161.
- [4] M. J. Yu, *Eng. Mater. Technol.* **2004**, 126, 271.
- [5] J. Chen, M. A. Hamon, H. Hu, Y. Chen, A. M. Rao, P. C. Eklund, R. C. Haddon, *Science* **1998**, 282, 95.
- [6] J. Chen, A. M. Rao, S. Lyuksyutov, M. E. Itkis, M. A. Hamon, H. Hu, R. W. Cohn, P. C. Eklund, D. T. Colbert, R. E. Smalley, R. C. Haddon, *J. Phys. Chem. B* **2000**, 105, 2525.
- [7] J. E. Riggs, D. B. Walker, D. L. Carroll, Y. Sun, *J. Phys. Chem. B* **2000**, 104, 7071.
- [8] D. W. Schaefer, J. M. Brown, D. P. Anderson, J. Zhao, K. Chokalingam, D. Tomlin, J. Ilavsky, *J. Appl. Cryst.* **2003**, 36, 553.

- [9] O. Matarredona, H. Rhoads, Z. Li, J. H. Harwell, L. Balzano, D. E. Resasco, *J. Phys. Chem. B* **2003**, *107*, 13357.
- [10] M. F. Islam, E. Rojas, D. M. Bergey, A. T. Johnson, A. G. Yodh, *Nano. Lett.* **2003**, *3*, 2.
- [11] S. Ramesh, L. M. Ericson, V. A. Davis, R. K. Saini, C. Kittrell, M. Pasquali, W. E. Billups, W. W. Adams, R. H. Hauge, R. E. Smalley, *J. Phys. Chem. B* **2004**, *108*, 8794.
- [12] K. D. Ausman, R. Piner, O. Lourie, R. S. Ruoff, *J. Phys. Chem. B* **2000**, *104*, 8911.
- [13] Y. Maeda, S. Kimura, Y. Hirashima, M. Kanda, Y. Lian, T. Wakahara, T. Akasaka, T. Hasegawa, H. Tokumoto, T. Shimizu, H. Kataura, Y. Miyauchi, S. Maruyama, S. Kobayashi, S. Nagase, *J. Phys. Chem. B* **2004**, *108*, 18395.
- [14] Y. Sun, S. R. Wilson, D. I. Schuster, *J. Am. Chem. Soc.* **2001**, *123*, 5348.
- [15] H. Kitano, K. Tachimoto, M. Gemmei-Ide, N. Tsubaki, *Macromol. Chem. Phys.* **2006**, *207*, 812.
- [16] C. A. Mitchell, J. L. Bahr, S. Arepalli, J. M. Tour, R. Krishnamoorti, *Macromolecules* **2002**, *35*, 8825.
- [17] E. J. Siochi, D. C. Working, C. Park, P. T. Lilehei, J. H. Rouse, C. C. Topping, A. R. Bhattacharyya, S. Kumar, *Compos. Part B: Eng* **2004**, *35*, 439.
- [18] P. Pötschke, A. R. Bhattacharyya, A. Janke, S. Pegel, A. Leohardt, C. Taschner, M. Ritschel, S. Roth, B. Hornbostel, *Fullerenes Nanotubes Carbon Nanostruct.* **2005**, *13*, 211.
- [19] S. Barrau, P. Demont, C. Maraval, A. Bernes, C. Lacabanne, *Macromol. Rapid Commun.* **2005**, *26*, 390.
- [20] Y. J. Kim, T. S. Shin, H. D. Choi, J. H. Kwon, Y. Chung, H. G. Yoon, *Carbon* **2005**, *43*, 23.
- [21] M. S. P. Shaffer, A. H. Windle, *Adv. Mater.* **1999**, *11*, 937.
- [22] X. Gong, J. Liu, S. Baskaran, R. D. Voise, J. S. Young, *Chem. Mater.* **2000**, *12*, 1049.
- [23] H. G. Chae, T. V. Sreekumar, T. Uchida, S. Kumar, *Polymer* **2005**, *46*, 10925.
- [24] T. Chatterjee, K. Yurekli, V. G. Hadjiev, R. Krishnamoorti, *Adv. Funct. Mater.* **2005**, *15*, 1832.
- [25] D. Yu, J. H. An, J. Y. Bae, Y. E. Lee, S. D. Ahn, S. Kang, K. S. Suh, *J. Appl. Polym. Sci.* **2004**, *92*, 2970.
- [26] B. Erdem, E. D. Sudol, V. L. Dimonie, M. S. El-Aasser, *J. Polym. Sci., Part A: Polym. Chem.* **2000**, *38*, 4419.
- [27] Q. Wang, H. Xia, C. Zhang, *J. Appl. Polym. Sci.* **2001**, *80*, 1478.
- [28] Y. Yang, X. Z. Kong, C. Y. Kan, C. G. Sun, *Polym. Adv. Technol.* **1999**, *10*, 54.
- [29] Z. Zeng, J. Yu, Z. Guo, *Macromol. Chem. Phys.* **2005**, *206*, 1558.
- [30] S. Lelu, C. Novat, C. Graillat, A. Guyot, E. Bourgeat-Lami, *Polym. Int.* **2003**, *52*, 542.
- [31] T. Batzilla, A. Tulke, *J. Coat. Technol.* **1998**, *70*, 881.
- [32] H. Xia, Q. Wang, G. Qiu, *Chem. Mater.* **2003**, *15*, 3879.
- [33] X. Xia, G. Qiu, Q. Wang, *J. Appl. Polym. Sci.* **2006**, *100*, 3123.
- [34] F. Tiarks, K. Landfester, M. Antonietti, *Macromol. Chem. Phys.* **2001**, *202*, 51.
- [35] H. J. Barraza, F. Pompeo, E. A. O'Rear, D. E. Resasco, *Nano Lett.* **2002**, *2*, 797.
- [36] H. T. Ham, Y. S. Choi, M. G. Chee, I. J. Chung, *J. Polym. Sci., Part A: Polym. Chem.* **2006**, *44*, 573.
- [37] J. C. Grunlan, W. W. Gerberich, L. F. Francis, *J. Appl. Polym. Sci.* **2001**, *80*, 692.
- [38] J. C. Grunlan, W. W. Gerberich, L. F. Francis, *Polym. Eng. Sci.* **2001**, *41*, 1947.
- [39] J. C. Grunlan, A. R. Mehrabi, M. V. Bannon, J. L. Bahr, *Adv. Mater.* **2004**, *16*, 150.
- [40] O. Regev, P. N. B. Elkati, C. E. Koning, *Adv. Mater.* **2004**, *16*, 248.
- [41] A. Dufresne, M. Paillet, J. L. Putaux, R. Canet, F. Carmona, P. Delhaes, S. Cui, *J. Mat. Sci.* **2002**, *37*, 3915.
- [42] <http://www.swnano.com/technology/pages.asp?mod=1&pg=1>.
- [43] G. Lolli, L. Zhang, L. Balzano, N. Sakulchaicharoen, Y. Tan, D. E. Resasco, *J. Phys. Chem. B* **2006**, *110*, 2108.
- [44] Y. Tan, D. E. Resasco, *J. Phys. Chem. B* **2005**, *109*, 14454.
- [45] F. Du, R. C. Scogna, W. Zhou, S. Brand, J. E. Fischer, K. I. Winey, *Macromolecules* **2004**, *37*, 9048.
- [46] E. J. Garboczi, K. A. Snyder, J. Douglas, *Phys. Rev. E.* **1995**, *52*, 819.
- [47] D. S. McLachlan, C. Chiteme, C. Park, K. E. Wise, S. E. Lowther, P. T. Lilehei, E. J. Siochi, J. S. Harrison, *J. Polym. Sci., Part B: Polym. Phys.* **2005**, *43*, 3273.
- [48] M. R. Piggott, "Load-Bearing Fibre Composites", Pergamon, 1980, Chapter 4, pp. 79.
- [49] P. Pötschke, T. D. Fomes, D. R. Paul, *Polymer* **2002**, *43*, 3247.
- [50] P. Pötschke, A. R. Bhattacharyya, A. Janke, *Polymer* **2003**, *44*, 8061.
- [51] P. Pötschke, M. Abdel-Goad, I. Alig, S. Dudkin, D. Lellinger, *Polymer* **2004**, *45*, 8863.
- [52] M. Abdel-Goad, P. Pötschke, *J. Non-Newt. Fluid Mech.* **2005**, *128*, 2.
- [53] X. Shi, J. L. Hudson, P. Spicer, J. M. Tour, R. Krishnamoorti, A. G. Mikos, *Nanotechnology* **2005**, *16*, S531.
- [54] T. Chatterjee, K. Yurekli, V. G. Hadjiev, R. Krishnamoorti, *Adv. Funct. Mater.* **2005**, *15*, 1838.
- [55] A. Eisenberg, B. Hird, R. B. Moore, *Macromolecules* **1990**, *23*, 4098.
- [56] "Polymer Handbook", J. Brandrup, E. H. Immergut, E. Grulke, Eds., 4th edition, John Wiley & Sons, New York 1999.